Rapid stress relaxation and degradable aromatic disulfide vitrimer for recyclable carbon fiber reinforced composite

Qinghua Zhang
Mingzhuan Li
Peifeng Feng
Luoli Meng
Xigao Jian
Jian Xu
xujian1028@dlut.edu.cn

Dalian University of Technology https://orcid.org/0000-0003-2542-1971

Research Article

Keywords: amine-catalyzed, aromatic disulfide vitrimer, rapid stress relaxation, degradation

Posted Date: November 29th, 2023

DOI: https://doi.org/10.21203/rs.3.rs-3654116/v1

Version of Record: A version of this preprint was published at Journal of Polymer Research on March 4th, 2024. See the published version at https://doi.org/10.1007/s10965-024-03939-z.

Abstract

Carbon fiber thermoset composites pose significant challenges due to their inability to be reprocessed and the difficulties in recycling carbon fibers. Vitrimer materials with reversible dynamic covalent bonding offer a promising solution for the degradation of thermosetting resins and the recycling of carbon fibers. However, their practical application is limited by inability to quickly release stresses from deformation and long degradation times. To address these limitations, this study presents a novel vitrimer material based on free amine-catalyzed aromatic dynamic disulfide exchange. The dynamic disulfide exchange network, catalyzed by free amines, exhibits rapid stress relaxation, with a relaxation time of only 14 s at 180°C. This exceptional dynamic exchange capability grants the vitrimer material outstanding self-healing properties, shape memory functionality, and recycling performance. Moreover, the higher concentration of disulfide bonds and the generation of small molecules increase the susceptibility of the crosslinked network to thiol degradation, resulting in resin degradation within 5 h. Additionally, this research successfully applies the vitrimer material as a matrix to prepare carbon fiber composites with exceptional mechanical properties. Furthermore, by degrading the resin matrix, effective recycling of carbon fibers is achieved, contributing to sustainable practices in the automotive and aerospace industries.

1. Introduction

Carbon fiber reinforced thermoset resin matrix composites are extensively utilized in sports equipment, automotive, aerospace, and other fields due to their advantageous properties such as low specific gravity, low coefficient of expansion, high heat resistance, and exceptional mechanical performance [1–6]. Thermoset resin matrices often have excellent solvent resistance, corrosion resistance, and high mechanical properties [7, 8]. However, the permanent cross-linked structure and non-melting, insoluble characteristics prevent thermoset resins from being healed, reprocessed, or degraded once fully cured [9, 10]. Presently, waste thermosetting resins are predominantly disposed of through incineration and landfilling, leading to environmental pollution and resource wastage [11–13]. Therefore, addressing the challenges associated with the self-healing, recycling, and degradation of thermosetting resins is importance.

The development of Covalent Adaptable Networks (CANs) has addressed the challenges related to the self-healing, recycling, and degradation of thermoset resins [14–16]. In 2011, Leibler et al. introduced "Vitrimer" materials [17], a class of polymers with reversible dynamic covalent bonds (such as ester exchange [18–20], alkyl exchange [21, 22], disulfide bonds [23, 24], boronic ester bonds [25, 26], olefin metathesis [27], etc.). These materials maintain permanent covalent networks and demonstrate excellent solvent resistance and dimensional stability through dynamic covalent bond exchange.

With the further development of vitrimer materials, a number of dynamic covalent bonds are expected to enable the degradation of the material. Ester-exchange based vitrimer materials can be degraded by hydroxyl-ester exchange, but the ester-exchange reaction often requires the addition of additional

catalysts, some of which lead to reduced mechanical properties and higher costs [28, 29]. Imine-exchange based vitrimer materials can be degraded by imine-imine exchange, but imine-based vitrimer is more sensitive to the environment and tends to decompose in environments with high water content, making it difficult to use in complex environments with harsh conditions [30, 31]. Aromatic disulfide vitrimer materials offer the potential for degradation through thiol-disulfide exchange reactions. These materials often exhibit excellent mechanical properties and environmental stability due to their rigid benzene ring structure and stable chemical bonds [32, 33]. However, aromatic disulfide vitrimer materials still have many limitations. Firstly, the rapid release of stresses generated by deformation remains a challenge. For instance, Si et al. proposed an epoxy vitrimer with high disulfide bonding but a relaxation time of over 1 min at 180°C [24], while Tang et al. developed a vitrimer with disulfide bonds from a new epoxy resin, exhibiting a stress relaxation time of 27.5 s at 200°C [34]. Secondly, disulfide-bonded resins still exhibit long degradation times. Tang et al. achieved complete degradation of disulfide-exchanged vitrimer material immersed in a DMF solution of β-mercaptoethanol (β-ME) after 7 days (DMF : β-ME = 5:5) [34]. Similarly, Alaitz et al. achieved degradation of epoxy resins based on disulfide exchange using a DMF solution of 2-thioethanol after 24 h [35]. Hence, a significant challenge lies in developing a simple method to prepare aromatic disulfide vitrimer materials with rapid stress relaxation and degradation properties.

In this paper, the addition of different contents of 4–4' diaminodiphenyl disulfide (AFD) as a curing agent and catalyst was chosen to introduce free amino groups and higher concentrations of S-S bonds in the vitrimer system, which can act as catalysts. The addition of the catalyst reduces the activation energy of the dynamic disulfide exchange and rapidly releases the deformation stresses, while the higher concentration of disulfide bonds and the smaller molecules in the system accelerate the degradation of the vitrimer material. Vitrimer material (GTE-AFD$_{1.25}$) exhibits excellent thermodynamic stability and mechanical properties. At the same time the vitrimer has a short relaxation time and can quickly release the stresses generated by deformation, allowing the material to exhibit self-healing, shape memory and recycling properties. The vitrimer can undergo successful degradation through the exchange reaction between disulfide bonds and thiols. In addition, carbon fiber reinforced composite (GTE-AFD$_{1.25}$-CF) was further prepared and investigated for its mechanical properties, shape memory properties and effective recycling of carbon fibers.

2. Experimental

2.1 Materials

4-Aminophenyl disulfide (AFD, ≥ 98%), N, N-Dimethylformamide (DMF) and 1,4-Dithiothreitol (DTT) were purchased from Aladdin Reagent. Glycerol triglycidyl ether (GTE, 143–154 g/eq) was purchased from Macklin, Plain weave filament carbon fiber fabric (3 K) was obtained from Dongli Carbon Fiber Co., Ltd.

2.2 Preparation of GTE-AFD vitrimers

Different amounts of GTE and AFD were uniformly mixed at 50 ℃ to obtain the initial crosslinking mixture, with specific ratios as shown in Table 1. The mixture was then poured into a polytetrafluoroethylene mold and cured it in a vacuum oven. The curing procedure involved sequential curing steps: 80°C for 2 h, 100°C for 2 h, 120°C for 2 h and 140°C for 2 h.

Table 1
Formulas of the GTE-AFD vitrimers.

Sample	Ratio[a)]	GTE (g)	Epoxy group content (mol)	AFD (g)	Active hydrogen group content (mol)
GTE-$AFD_{0.75}$	0.75	10	0.065	3.042	0.049
GTE-$AFD_{1.00}$	1.00	10	0.065	4.036	0.065
GTE-$AFD_{1.25}$	1.25	10	0.065	5.029	0.081
GTE-$AFD_{1.50}$	1.50	10	0.065	6.085	0.098

[a)] Ratio = active hydrogen group content/epoxy group content.

2.3 Preparation of GTE-$AFD_{1.25}$-CF vitrimers.

A well-mixed resin solution was prepared by combining 20.00 g of GTE and 10.06 g of AFD in a flask and stirring at 50°C until homogeneity was achieved. Carbon fiber-reinforced resin-based composites were fabricated using a vacuum infusion method [36, 37]. The composites were subsequently cured in a vacuum oven using a stepwise curing process: 80°C for 2 h, 100°C for 2 h, 120°C for 2 h and 140°C for 2 h.

2.4 Characterization

The GTE-AFD vitrimers were subjected to Fourier-transform infrared (FTIR) spectroscopy using a potassium bromide pellet method. The FTIR analysis was performed using an Invenio R instrument from Bruker Technology Co., Germany. The resolution was set to 2 cm^{-1}, and the wavenumber range scanned was from 400 to 4000 cm^{-1}. The spectra were collected with 32 scans.

The immersion method was used to measure the gel fraction of the samples. The non-cross-linked portions were removed by immersing the sample (W_1, ~ 1 g) in 25 mL of acetone for 24 h at room temperature. The insoluble portions were dried in an oven at 60°C to a constant weight (W_2) for 12 h. The gel fractions (G_f) were obtained according to the equation

$$G_f = \frac{W_2}{W_1} \times 100\%$$

1

And the cross-linking density (ρ) of vitrimers is obtained according to the Flory's ideal rubber elasticity theory as follows:

$$\rho = \frac{E''}{3RT}$$

2

Where ρ is the cross-linking density of vitrimers; E'' is the storage modulus at (T_g+30) ℃; R represents the gas constant, and the T is the absolute temperature of (T_g+30) ℃.

The degree of cure and glass transition temperature of GTE-AFD vitrimers were tested using a differential scanning calorimeter (DSC 250) from TA Instruments, USA. The testing was conducted under a nitrogen (N_2) protective atmosphere, with a temperature range of 25°C to 150°C and a heating rate of 5°C min^{-1}.

The dynamic mechanical properties of GTE-AFD vitrimers were tested using a Dynamic Mechanical Analyzer (DMA Q850) from TA Instruments, USA. The following testing conditions were applied: sample dimensions of 35 mm × 12 mm × 2 mm, a single cantilever testing fixture, a fixed frequency of 1 Hz, and a heating rate of 3°C min^{-1} from 0°C to 150°C to measure the changes in storage modulus and loss factor. The stress relaxation behavior of GTD-AFD vitrimer was tested using a DMA Q850. The samples were subjected to different testing temperatures and held for 5 min, with a strain of 1%.

The thermal decomposition temperature of GTE-AFD vitrimer was measured using a simultaneous thermal analyzer (STA 449F3) from Netzsch Instrument Group, Germany. The testing was performed under a nitrogen (N_2) protective atmosphere, with a temperature range of 50°C to 1000°C and a heating rate of 10°C min^{-1}.

Conducted a three-point flexural test using a universal testing machine (Zwick/Roell Z250AF, Ulm, Germany) at room temperature and atmospheric pressure. The dimensions of the specimens were 35 mm × 12.7 mm × 2 mm, with an external loading rate of 2 mm min^{-1} and a specimen span of 32 mm. Each sample was tested five times, and the flexural strength was calculated according to formula (3).

$$\sigma = \frac{3FL}{2bh^2}$$

3

σ - flexural strength (MPa), F - maximum load (N), L - span length (mm), b - width of specimen (mm), h - thickness of specimen (mm).

A uniaxial tensile test was conducted at room temperature using a universal testing machine (Zwick/Roell Z250AF, Ulm, Germany). Dumbbell-shaped specimens with dimensions of 100 mm × 25 mm × 2 mm were used, and the tensile rate was set to 1 mm min^{-1}. Each sample was tested five times, and the tensile strength was calculated according to formula (4).

$$\sigma = \frac{F}{S}$$

4

σ - tensile strength (N), F - axial tensile force (N), S - cross-sectional area of the specimen (mm^2).

To assess the self-healing, a crack was made on the surface of the resin using a blade, followed by healing at 140°C. The healing progress of the crack at different healing times was observed using a metallographic microscope (Axiolab 5) from Carl Zeiss, Germany.

The shape memory performance of GTE-$AFD_{1.25}$ vitrimer was studied by applying external force to bend it into different shapes at 120°C and 180°C.

To assess the recyclability of GTE-$AFD_{1.25}$, it was cut into small pieces and hot-pressed to obtain reshaped GTE-$AFD_{1.25}$ samples. The mechanical properties of the restructured resin were then investigated using a Zwick universal testing machine in a three-point flexural test.

GTE-AFD vitrimers and GTE-$AFD_{1.25}$-CF were immersed in a dithiothreitol (DTT) solution in dimethylformamide (DMF) and observed for degradation at 90°C.

The surface morphology of GTE-$AFD_{1.25}$-CF and carbon fibers before and after recycling was observed using a scanning electron microscope (SEM Regulus 8230) from Hitachi, Japan.

Raman spectroscopy was performed using a Raman imaging microscope (Thermo Fisher Scientific) with a 532 nm laser wavelength. The laser power was adjusted to 12 mW and the exposure time was set to 60 s.

The mechanical properties of individual carbon fibers were assessed using a single fiber testing instrument (FAVIMAT+, TEXTECHNO, Germany) before and after the recycling process.

3. Results and discussions

3.1 Dynamic disulfide bond exchange mechanism

Different ratios of the curing agent AFD were used to cure GTE, resulting in GTE-AFD vitrimers with a dynamic disulfide covalent network, as shown in Fig. 1a. The traditional aromatic disulfide exchange reaction mechanism is mediated through a [2 + 1] radical-mediated mechanism [38, 39], as shown in

Fig. 1b. In this mechanism, S-S bond cleavage generates a methylthiyl radical, which can attack another disulfide bond on a different chain, leading to the formation of a new radical and another disulfide compound in a single substitution reaction. Through the radical-mediated mechanism, under thermal stimulation, the disulfide bonds in the GTE-AFD vitrimer material undergo cleavage and rearrangement. Furthermore, in the presence of nucleophilic agents in the polymer system, the coupling exchange of disulfide bonds can be catalyzed, accelerating the rearrangement of the crosslinked network [40]. Figure 1c illustrates the amino-catalyzed dynamic disulfide exchange mechanism The lone pair electrons in the amino group create a nucleophilic intermediate with the sulfur atom, which subsequently forms a three-membered cyclic transition state with the disulfide bond. In this process, the electron density on the sulfur atom changes, leading to a reduction in the energy of the disulfide bond, thereby accelerating the dynamic exchange of disulfide bonds.

3.2 Characterization of thermal properties

The structure of GTE-AFD vitrimers were analyzed using FTIR, as depicted in Fig. 2a. At 910 cm^{-1}, the characteristic peaks of epoxy disappear in GTE-$AFD_{1.00}$, GTE-$AFD_{1.25}$, and GTE-$AFD_{1.50}$, indicating complete polymer curing. Compared to GTE-$AFD_{0.75}$ and GTE-$AFD_{1.00}$, GTE-$AFD_{1.25}$ and GTE-$AFD_{1.50}$ exhibit two new absorption peaks at 1291 cm^{-1} and 1323 cm^{-1} (aromatic amine C-N stretching vibration), indicating the presence of free amino groups in the polymer system. From the DSC testing data (Fig. S1), it can be observed that there is no significant exothermic peak as the temperature increases, indicating complete curing of the resin. TGA testing was employed to evaluate the thermal stability of the polymer, which is an important parameter for the application of thermosetting resins. From Fig. 2b, it can be seen that the temperature at which GTE-AFD vitrimers exhibit 5% weight loss when the temperature is above 240°C. This indicates that GTE-AFD vitrimers exhibits good thermal stability. Figure 2c illustrates that below T_g, the vitrimers exhibits high rigidity with a storage modulus between 2000 MPa and 3000 MPa. Beyond T_g, the vitrimers transitions to a rubbery state, causing a rapid storage modulus decline, ultimately relaxing to 0 MPa as polymer chains gain mobility. T_g can be determined by analyzing the peak of tan δ in DMA testing (Fig. 2d). The T_g of GTE-AFD vitrimers increases from 72.49°C to 102.79°C as the stoichiometric ratio of AFD increases, which is attributed to the rigid hexagonal structure in AFD that restricts the segmental motion of the polymer chains [41, 42]. The cross-link density of GTE-AFD vitrimers was calculated according to Flory's ideal rubber elasticity theory (Fig. S2). With the increase of AFD content, the cross-link density of vitrimers first increased and then decreased (1.38×10^{-3} mol cm^{-3} → 1.76×10^{-3} mol cm^{-3}→ 1.39×10^{-3} mol), and GTE-$AFD_{1.00}$ and GTE-$AFD_{1.25}$ exhibited higher cross-link densities. The gel fraction was also tested (Table 2), which is proportional to the cross-link density of the network. The gel fraction of GTE-$AFD_{1.25}$ was 99.9 ± 0.1, confirming that GTE-$AFD_{1.25}$ has the highest cross-link density.

GTE-AFD vitrimers were tested for mechanical properties. Tensile strength (Fig. 3a) and Young's modulus (Fig. 3b) increase with an increase in rigid benzene ring structure and cross-link density. The flexural strength (Fig. 3c) and flexural modulus (Fig. 3d) of the vitrimers also increase, reaching the highest

values at GTE-AFD$_{1.25}$. GTE-AFD$_{0.75}$ and GTE-AFD$_{1.50}$ have lower mechanical properties due to lower crosslink density. Both GTE-AFD$_{1.00}$ and GTE-AFD$_{1.25}$ demonstrate high mechanical performance. GTE-AFD$_{1.25}$ exhibits the highest mechanical properties due to high crosslink density and rigid conjugate structure (Table 2). Higher mechanical properties compared to reported biodegradable vitrimer materials.

Table 2
Cross-link Density, Gel Content, Dynamic Mechanical Parameters, and Mechanical Property of GTE-AFD Vitrimers.

Sample	Cross-link density (10^{-3} mol cm^{-3})	Gel fraction(%)	E^0 (0 °C) (MPa)	T_g (°C)	T_d (°C)	Tensile stress/modulus (MPa)	Flexural stress/modulus (MPa)
GTE-AFD$_{0.75}$	1.38	99.6±0.3	2552	72.49	265	73.74/2652	95.93/2340
GTE-AFD$_{1.00}$	1.64	99.8±0.1	3038	95.40	264	85.94/3056	135.17/2760
GTE-AFD$_{1.25}$	1.76	99.9±0.1	2793	99.27	258	94.62/3151	157.16/2970
GTE-AFD$_{1.50}$	1.39	99.6±0.2	2448	102.79	243	76.38/2741	123.99/2380

The mechanical performance of GTE-AFD$_{0.75}$ and GTE-AFD$_{1.50}$ is significantly reduced, limiting their application in complex environments. Therefore, further investigation was conducted to explore the effect of introducing free amino groups on the stress relaxation time of the polymer, focusing on GTE-AFD$_{1.25}$ and GTE-AFD$_{1.00}$.

3.3 GTE-AFD vitrimers network rearrangement characteristics

The stress relaxation phenomenon is the result of dynamic structural exchange and network rearrangement in vitrimer networks. The topological network rearrangement of GTE-AFD vitrimers were studied through stress relaxation experiments. The relaxation time refers to the duration required for the modulus or stress to decrease to 1/e (36.8%) of its initial value [43, 44]. Figure 4a and 4c present the stress relaxation behavior of GTE-AFD$_{1.00}$ and GTE-AFD$_{1.25}$ vitrimers, respectively, at temperatures of 120°C, 140°C, 160°C, and 180°C.

As the temperature went from 120 °C to 180 °C, the GTE-AFD$_{1.00}$ relaxation time decreased from 2888 s to 30 s, while GTE-AFD$_{1.25}$ went from 1066 s to 14 s. Compared to GTE-AFD$_{1.00}$, GTE-AFD$_{1.25}$ exhibits a

faster relaxation rate at all temperatures. This is because the free amino groups in the polymer system serve as internal catalysts, promoting the exchange of disulfide bonds, thereby increasing the exchange rate of dynamic disulfide bonds in the system and reducing the relaxation time of the polymer.

The relaxation process of vitrimer materials follows the Maxwell model fitted by the Arrhenius equation, as shown in formula 5 [19, 45]. In the given equation, R is the gas constant, τ represents the stress relaxation time, and A is the pre-exponential factor.

$$ln\tau = \frac{Ea}{RT} - lnA$$

5

Figure 4b and Fig. 4d show the Arrhenius equation fit curve for the stress relaxation time τ of GTE-AFD$_{1.00}$ and GTE-AFD$_{1.25}$. The stress relaxation activation energies of GTE-AFD$_{1.00}$ and GTE-AFD$_{1.25}$ are calculated to be 111.86 kJ mol^{-1} and 105.88 kJ mol^{-1}. GTE-AFD$_{1.25}$ has a lower activation energy, and this lower activation energy will greatly facilitate topological rearrangements for rapid exchange reactions.

3.4 Self-healing, triple-shape memory, and recycling performance of GTE-AFD$_{1.25}$ vitrimer

The GTE-AFD$_{1.25}$ vitrimer exhibits a faster dynamic disulfide exchange rate. Therefore, further investigation was conducted on the self-healing, triple-shape memory, and recycling performance of GTE-AFD$_{1.25}$. Figure 5a shows the study on the self-healing performance of GTE-AFD$_{1.25}$. Scratches were made on the surface of GTE-AFD$_{1.25}$ using a knife, and the material was heated at 140°C in a vacuum oven. After heating for 30 min, the scratch depth decreased from 112.75 μm to 4.23 μm (recovery rate of 96.25%), indicating a rapid healing speed. After heating for 60 min, the scratch depth further reduced to 4.17 μm (recovery rate of 96.30%), but with a slower healing speed. Overall, GTE-AFD$_{1.25}$ demonstrates excellent healing efficiency and a relatively fast healing rate.

Figure 5b illustrates the investigation of its shape memory performance. GTE-AFD$_{1.25}$ exhibits triple-shape memory properties. A temporary "U" shape is obtained by applying an external force to the rectangular sample at 120°C and removing the force to return to room temperature. When heated again to 120°C, the "U" shape returns to a permanent rectangle, exhibiting T_g-based shape memory properties. A "permanent" "U" shape is obtained by applying an external force to the rectangular sample at 180°C and holding it for 30min, then removing the force and returning it to room temperature. The sample was then bent into a "S" shape at 120°C. A temporary "S" shape is then obtained by removing the external force and returning to room temperature. Further, the sample returns from a temporary "S" shape to a "permanent" "U" shape when heated to 120°C. Finally, as the temperature increased to 180°C, it reverted from the "U" shape to the original permanent rectangular shape. The dynamic exchange of S—S bonds and

topological rearrangement occurred in the crosslinked network of GTE-$AFD_{1.25}$, exhibiting triple-shape memory properties.

The recycling performance of GTE-$AFD_{1.25}$ were further investigated by hot pressing the material cut into pieces at 180°C and 15 MPa. The fragments could be reprocessed into a rectangular shape, as shown in Fig. 5c. Mechanical performance testing was conducted on the samples before and after recycling, obtaining stress-strain curves for three-point flexural, as illustrated in Fig. 5d. The flexural strength of GTE-$AFD_{1.25}$ after hot pressing recycling was 116 MPa, and the reprocessed flexural performance reached 73.8% of the original GTE-$AFD_{1.25}$, indicating good mechanical properties even after recycling.

3.5 Degradation properties of GTE-AFD vitrimers

Crosslinked networks based on disulfide bonds possess reversible properties, and the thiol-disulfide exchange reaction can disrupt the crosslinking of polymers, leading to degradation of the resin in the presence of thiols [32, 46]. The degradation performance of GTE-$AFD_{1.00}$ and GTE-$AFD_{1.25}$ was studied as shown in Fig. 6a and 6b. At 90°C, GTE-$AFD_{1.00}$ and GTE-$AFD_{1.25}$ were placed in a DTT/DMF solution with a concentration of 0.2 g L^{-1}. After 5 h, partial degradation of GTE-$AFD_{1.00}$ was observed, while GTE-$AFD_{1.25}$ completely degraded. Under the same conditions, GTE-$AFD_{1.25}$ exhibited a faster degradation rate due to two main reasons. Firstly, GTE-$AFD_{1.25}$ had a higher content of disulfide bonds compared to GTE-$AFD_{1.00}$, making it more susceptible to exchange reactions with external free thiols, resulting in rapid degradation of the crosslinked network. Secondly, the highly crosslinked GTE-$AFD_{1.00}$ degraded into linear polymers (Fig. 6c), while the GTE-$AFD_{1.25}$ polymer system contained unreacted free amines that were more easily degraded into small molecules during degradation (Fig. 6d). Decomposition into small molecules is more effective for the degradation and dissolution of thermosetting materials [47]. Therefore, GTE-$AFD_{1.25}$ exhibited a faster degradation rate. Higher disulfide bonds content and generation of small molecules accelerated the degradation rate of the crosslinked network in GTE-$AFD_{1.25}$, effectively addressing the challenge of recycling thermosetting resins.

3.6 Mechanical, reprocessing and shape memory properties of GTE-$AFD_{1.25}$-CF and recycling of carbon fibers

GTE-$AFD_{1.25}$ is used as a matrix for the preparation of carbon fiber reinforced composites because of its rapid release of deformation-generated stresses and its excellent mechanical properties. The surface morphology of carbon fibers and GTE-$AFD_{1.25}$-CF composite were observed by SEM, as shown in Fig. S3. After incorporating GTE-$AFD_{1.25}$ matrix, GTE-$AFD_{1.25}$ was uniformly distributed on the surface of carbon fiber, indicating good interfacial bonding in the composite. Furthermore, the mechanical properties of GTE-$AFD_{1.25}$-CF were investigated through three-point flexural experiments. The flexural strength of GTE-$AFD_{1.25}$-CF was 721 MPa, and the flexural modulus was 3.03 GPa, the composite has excellent mechanical properties. (Fig. S4).

Traditional thermosetting composites possess a permanent crosslinked structure and lack reprocessing capabilities, which greatly limits their applications in certain environments. However, GTE-AFD$_{1.25}$ can undergo topological rearrangement at a certain temperature. By using it as a composite matrix and introducing dynamic disulfide bonds, the composite becomes reprocessable. As shown in Fig. S5, The GTE-AFD$_{1.25}$-CF was subjected to a thermal treatment at 180°C, where it was bent into a "√" shape and maintained in this configuration for a duration of 30 min. The dynamic crosslinked network underwent topological rearrangement at high temperature, resulting in a permanent "√" shape while maintaining great mechanical performance, capable of supporting a weight of 546 g (approximately 1000 times its own weight). This indicates that the composite retains excellent mechanical properties even after reprocessing. Additionally, the composite also exhibits shape memory performance based on the resin's T_g (Fig. S6). A "U" shape was obtained by applying an external force to the rectangular composite at 120°C. Upon return to room temperature, the composite retained its temporary "U" shape. Subsequently, upon raising the temperature back to 120°C, the composite restored its permanent rectangular shape.

The degradation process of GTE-AFD$_{1.25}$-CF was illustrated in Fig. 7a. When placed in a DTT/DMF solution, the resin matrix completely separated from the fibers after 5 h. SEM analysis was performed to investigate the surface morphology of carbon fibers before and after recycling, as illustrated in Fig. 7b. The recycled carbon fibers exhibited a clean and smooth surface, nearly identical to the original carbon fibers, indicating that the resin had degraded almost completely. A comparison of the chemical structures of the carbon fiber surfaces original and after recycled was conducted, as depicted in Fig. 7c. The Raman spectra of the carbon fibers were identical before and after recycling, indicating that the degradation process did not affect the chemical structure of the carbon fibers. In addition, the mechanical properties of carbon fiber monofilaments original and after recycled were investigated, as illustrated in Fig. 7d. The tensile strength, fracture strain, and tensile modulus of the recycled carbon fibers were 2890 MPa, 1.39%, and 209.13 GPa, respectively, while those of the original carbon fibers were 3210 MPa, 1.39%, and 239.46 GPa, respectively. The mechanical properties of the carbon fibers were not significantly compromised following recycling, suggesting the continued suitability of recycled carbon fibers for the production of carbon fiber-reinforced composites. In summary, the GTE-AFD$_{1.25}$-CF can be effectively degraded by thiols while the recycled carbon fibers demonstrate comparable surface morphology, chemical structure, and mechanical properties to the original carbon fibers.

4. Conclusions

In this study, aromatic disulfide vitrimers with fast stress relaxation and rapid degradation were prepared by adding different contents of AFD as a curing agent and also as a catalyst. Among the compositions, GTE-AFD$_{1.25}$ vitrimer exhibited excellent properties, including a glass transition temperature of 99.27°C, high tensile and flexural strength (94.62 MPa and 157.16 MPa, respectively), and high modulus (3151 MPa and 2970 MPa, respectively). This vitrimer also demonstrated fast dynamic exchange of disulfide bonds (relaxation time of 14 s at 180°C), resulting in a high self-healing efficiency of 96.25%. It exhibited triple-shape memory and excellent reprocessing capabilities. Furthermore, the GTE-AFD$_{1.25}$ vitrimer

exhibited superior degradation performance compared to the uncatalyzed GTE-$AFD_{1.00}$ vitrimer, completely degrading in a DTT/DMF solution within 5 h. Carbon fiber-reinforced GTE-$AFD_{1.25}$-CF composites displayed outstanding mechanical properties, with a flexural strength of 721 MPa and a modulus of 30334 MPa. These composites also exhibited reprocessing, shape memory, and degradation capabilities, with effective recycling of the carbon fibers. Overall, our study presents a high-strength, multi-functional resin matrix and its carbon fiber composite, offering efficient degradation and recycling of carbon fibers, contributing to environmental sustainability and resource utilization.

Declarations

Author contributions Qinghua Zhang: Conceptualization, Methodology, Investigation, Formal analysis, Data curation, Visualization, Writing - Original draft preparation, Writing – Review & Editing. Mingzhuan Li: Visualization, Investigation. Peifeng Feng: Investigation, Methodology. Luoli Meng: Investigation, Methodology. Xigao Jian: Funding Acquisition, Supervision. Jian Xu (Corresponding Author): Conceptualization, Methodology, Funding Acquisition, Resources, Supervision, Writing - Review & Editing.

Data availability Data for the study is available upon reasonable request from the corresponding author.

Acknowledgements

This work was supported by the National Natural Science Foundation of China [grant number 52075526], the “Ningbo 3315 Plan Innovation Team” [grant number 2017A-28-C], the National Natural Science Foundation of China [grant number 91860204], the Fundamental Research Funds for the Central Universities [grant number DUT22-LAB605], the National Key Research and Development Program [grant number 2018YFB1107500], and the financial support from National Young Talents Program of China.

Conflict of interest The authors declare that they have no conflict of interest.

References

1. M.B.A. Tamez, I. Taha (2021) A review of additive manufacturing technologies and markets for thermosetting resins and their potential for carbon fiber integration, Addit. Manuf. 37: 101748.
2. Q. Wang, H. Ning, U. Vaidya, S. Pillay, L.-A. Nolen (2015) Development of a carbonization-in-nitrogen method for measuring the fiber content of carbon fiber reinforced thermoset composites, Compos Part a-Appl S. 73: 80–84.
3. M. Ziaee, J.W. Johnson, M. Yourdkhani (2022) 3D Printing of Short-Carbon-Fiber-Reinforced Thermoset Polymer Composites via Frontal Polymerization, ACS Appl. Mater. Inter. 14: 16694–16702.
4. P. Feng, L. Ma, G. Wu, X. Li, M. Zhao, L. Shi, M. Wang, X. Wang, G. Song (2020) Establishment of multistage gradient modulus intermediate layer between fiber and matrix via designing double 'rigid-

flexible' structure to improve interfacial and mechanical properties of carbon fiber/resin composites, Compos. Sci. Technol. Nov.10: 200.

5. P.F. Feng, G.J. Song, X.R. Li, H. Xu, L.Y. Xu, D.D. Lv, X. Zhu, Y.D. Huang, L.C. Ma (2021) Effects of different "rigid-flexible" structures of carbon fibers surface on the interfacial microstructure and mechanical properties of carbon fiber/epoxy resin composites, J. Colloid. Interf. Sci. 583: 13–23.
6. Sarkari-Oskuei E, Safavi-Mirmahalleh S-A, Sofla RLM, Roghani-Mamaqani H, Salami-Kalajahi M (2023) Synthesis of recyclable polyurethane-based pseudo-vitrimer: comparison of properties with conventional polyurethane. J Polym Res 30: 338.
7. M.C. Lagel, A. Pizzi, M.C. Basso, S. Abdalla (2015) Development and characterization of abrasive grinding wheels with a tannin-furanic resins matrix, Ind. Crop. Prod. 65: 343–348.
8. C. Sonnenfeld, H. Mendil-Jakani, R. Agogue, P. Nunez, P. Beauchene (2017) Thermoplastic/thermoset multilayer composites: A way improve the impact damage tolerance of thermosetting resin matrix to composites, Compos. Struct. 171: 298–305.
9. K. Adekunle, S.W. Cho, R. Ketzscher, M. Skrifvars (2012) Mechanical properties of natural fiber hybrid composites based on renewable thermoset resins derived from soybean oil, for use in technical applications, J. Appl. Polym. Sci. 124: 4530–4541.
10. S. Barré, T. Chotard, M.L. (1996) Benzeggagh, Comparative study of strain rate effects on mechanical properties of glass fibre-reinforced thermoset matrix composite, Compos. Part. A-Appl. S. 27: 1169–1181.
11. M.A. Lucherelli, A. Duval, L. Averous (2022) Biobased vitrimers: Towards sustainable and adaptable performing polymer materials, Prog. Polym. Sci. 127: 101515.
12. X. Liu, E. Zhang, Z. Feng, J. Liu, B. Chen, L. Liang (2021) Degradable bio-based epoxy vitrimers based on imine chemistry and their application in recyclable carbon fiber composites, J. Mater. Sci. 56: 15733–15751.
13. M. Li, G. Zhao, X. Liu, X. Xie, C. Zhang, H. Yu, X. Jian, Y. Song, J. Xu (2023) Self-healing interface of carbon fiber reinforced composites based on reversible hydrogen-bonded interactions, Compos. Commun. 40: 101631.
14. C. Cheng, J. Li, F. Yang, Y. Li, Z. Hu, J. Wang (2018) Renewable eugenol-based functional polymers with self-healing and high temperature resistance properties, J Polym Res. 25:57.
15. W. Zhang, Q. Zhou, C. Fang, L. You, X. Li, M. Liu, X. Dong, Y. Qi, B. Wang, W. Li (2022) Dynamic networks for polyimine with disulfide bond to obtain catalyst-free recyclability, multi-degradation and malleability, J Polym Res. 29:154.
16. B. Krishnakumar, R.V.S.P. Sanka, W.H. Binder, V. Parthasarthy, S. Rana, N. Karak: (2020) Vitrimers: Associative dynamic covalent adaptive networks in thermoset polymers, Chem. Eng. J. 385: 123820.
17. D. Montarnal, M. Capelot, F. Tournilhac, L. Leibler (2011) Silica-Like Malleable Materials from Permanent Organic Networks, Science 334: 965–968.
18. T. Liu, B. Zhao, J. Zhang (2020) Recent development of repairable, malleable and recyclable thermosetting polymers through dynamic transesterification, Polymer 194: 122392.

19. Y. Xu, S. Dai, L. Bi, J. Jiang, H. Zhang, Y. Chen (2022) Catalyst-free self-healing bio-based vitrimer for a recyclable, reprocessable, and self-adhered carbon fiber reinforced composite, Chem. Eng. J. 429: 132518.
20. Y. Xu, H. Zhang, S. Dai, S. Xu, J. Wang, L. Bi, J. Jiang, Y. Chen (2022) Hyperbranched polyester catalyzed self-healing bio-based vitrimer for closed-loop recyclable carbon fiber-reinforced polymers, Compos. Sci. Technol. 228: 109676.
21. B. Hendriks, J. Waelkens, J.M. Winne, F.E. Du Prez (2017) Poly(thioether) Vitrimers via Transalkylation of Trialkylsulfonium Salts, ACS Macro. Lett. 6: 930–934.
22. J. Huang, L. Zhang, Z. Tang, S. Wu, B. Guo (2018) Reprocessable and robust crosslinked elastomers via interfacial C-N transalkylation of pyridinium, Compos. Sci. Technol. 168: 320–326.
23. Y.-Y. Liu, J. He, Y.-D. Li, X.-L. Zhao, J.-B. Zeng (2020) Biobased, reprocessable and weldable epoxy vitrimers from epoxidized soybean oil, Ind. Crop. Prod. 153: 112576.
24. H. Si, L. Zhou, Y. Wu, L. Song, M. Kang, X. Zhao, M. Chen (2020) Rapidly reprocessable, degradable epoxy vitrimer and recyclable carbon fiber reinforced thermoset composites relied on high contents of exchangeable aromatic disulfide crosslinks, Compos. Pt. B-Eng. 19: 108278.
25. M. Chen, Y. Wu, B. Chen, A.M. Tucker, A. Jagota, S. Yang (2022) Fast, strong, and reversible adhesives with dynamic covalent bonds for potential use in wound dressing, P. Natl. Acad. Sci. USA. 119: e2203074119.
26. Y.M. Shi, Y.G. Hong, J.Y. Hong, A.Y. Yu, M.W. Lee, J.Y. Lee, M. Goh (2022) Bio-based boronic ester vitrimer for realizing sustainable and highly thermally conducting nanocomposites, Compos. Pt. B-Eng. 244: 110181.
27. Y.-X. Lu, F. Tournilhac, L. Leibler, Z. Guan (2012) Making Insoluble Polymer Networks Malleable via Olefin Metathesis, J. Am. Chem. Soc. 134: 8424–8427.
28. Y.Q. Wang, X.J. Cui, Q.Q. Yang, T.S. Deng, Y.X. Wang, Y.X. Yang, S.Y. Jia, Z.F. Qin, X.L. Hou (2015) Chemical recycling of unsaturated polyester resin and its composites via selective cleavage of the ester bond, Green. Chem. 17: 4527–4532.
29. Y. Xu, H. Ma, H. Zhang, S. Xu, X. Cheng, L. Bi, J. Jiang, Y. Chen (2023) A dual dynamic network self-healing bio-based vitrimer and its application in multiply recyclable carbon fiber reinforced polymers, Ind. Crop. Prod. 198: 116755.
30. Y.-Y. Liu, G.-L. Liu, Y.-D. Li, Y. Weng, J.-B. Zeng (2021) Biobased High-Performance Epoxy Vitrimer with UV Shielding for Recyclable Carbon Fiber Reinforced Composites, ACS Sustainable. Chem. Eng. 9: 4638–4647.
31. X. An, Y. Ding, Y. Xu, J. Zhu, C. Wei, X. Pan (2022) Epoxy resin with exchangeable diselenide crosslinks to obtain reprocessable, repairable and recyclable fiber-reinforced thermoset composites, React. Funct. Polym. 172: 105189.
32. F. Zhou, Z. Guo, W. Wang, X. Lei, B. Zhang, H. Zhang, Q. Zhang (2018) Preparation of self-healing, recyclable epoxy resins and low-electrical resistance composites based on double-disulfide bond exchange, Compos. Sci. Technol. 167: 79–85.

33. B. Krishnakumar, R.V.S.P. Sanka, W.H. Binder, C. Park, J. Jung, V. Parthasarthy, S. Rana, G.J. Yun (2020) Catalyst free self-healable vitrimer/graphene oxide nanocomposites, Compos. Pt. B-Eng. 184: 107647.
34. S. Tang, H. Lin, K. Dong, J. Zhang, C. Zhao (2023) Closed-loop recycling and degradation of guaiacol-based epoxy resin and its carbon fiber reinforced composites with S-S exchangeable bonds, Polym. Degrad. Stabil. 210: 110298.
35. A. Ruiz de Luzuriaga, R. Martin, N. Markaide, A. Rekondo, G. Cabanero, J. Rodriguez, I. Odriozola (2016) Epoxy resin with exchangeable disulfide crosslinks to obtain reprocessable, repairable and recyclable fiber-reinforced thermoset composites, Mater. Horiz. 3: 241–247.
36. A. Toldy, A. Pomazi, B. Szolnoki (2020) The effect of manufacturing technologies on the flame retardancy of carbon fibre reinforced epoxy resin composites, Polym. Degrad. Stabil. 174: 109094.
37. A. Hammami, B.R. Gebart (2010) Analysis of the vacuum infusion molding process, Polym. Composite. 21: 28–40.
38. J.M. Matxain, J.M. Asua, F. Ruiperez (2016) Design of new disulfide-based organic compounds for the improvement of self-healing materials, Phys. Chem. Chem. Phys. 18: 1758–1770.
39. A.R. de Rekondo, G. Solera, I. Azcarate-Ascasua, V. Boucher, H.J. Grande, A. Rekondo (2022) Chemical control of the aromatic disulfide exchange kinetics for tailor-made epoxy vitrimers, Polymer 239: 124457.
40. S. Nevejans, N. Ballard, J.I. Miranda, B. Reck, J.M. Asua (2016) The underlying mechanisms for self-healing of poly(disulfide)s, Phys. Chem. Chem. Phys. 18: 27577–27583.
41. F.C. Ji, X.D. Liu, D.K. Sheng, Y.M. Yang, (2020) Epoxy-vitrimer composites based on exchangeable aromatic disulfide bonds: Reprocessibility, adhesive, multi-shape memory effect, Polymer 197: 122514.
42. Q. Zhou, X.J. Zhu, W.H. Zhang, N. Song, L.Z. Ni (2020) Recyclable High Performance Epoxy Composites Based on Double Dynamic Carbon-Nitrogen and Disulfide Bonds, ACS Appl. Polym. Mater. 2: 1865–1873.
43. J.-H. Chen, X.-P. An, Y.-D. Li, M. Wang, J.-B. Zeng (2018) Reprocessible Epoxy Networks with Tunable Physical Properties: Synthesis, Stress Relaxation and Recyclability, Chinese J. Polym. Sci. 36: 641–648.
44. B.M. El-Zaatari, J.S.A. Ishibashi, J.A. Kalow (2020) Cross-linker control of vitrimer flow, Polym Chem-UK. 11: 5339–5345.
45. H. Deng, J. Ye, Z. Zu, Z. Lin, H. Huang, L. Zhang, X. Ye, H. Xiang (2023) Repairable, reprocessable and recyclable rigid silicone material enabled by dual dynamic covalent bonds crosslinking side-chain, Chem. Eng. J. 465: 143038.
46. J. Rong, J. Zhong, W. Yan, M. Liu, Y. Zhang, Y. Qiao, C. Fu, F. Gao, L. Shen, H. He (2021) Study on waterborne self-healing polyurethane with dual dynamic units of quadruple hydrogen bonding and disulfide bonds, Polymer 221: 123625.

47. A. Takahashi, T. Ohishi, R. Goseki, H. Otsuka (2016) Degradable epoxy resins prepared from diepoxide monomer with dynamic covalent disulfide linkage, Polymer 82: 319–326.

Figures

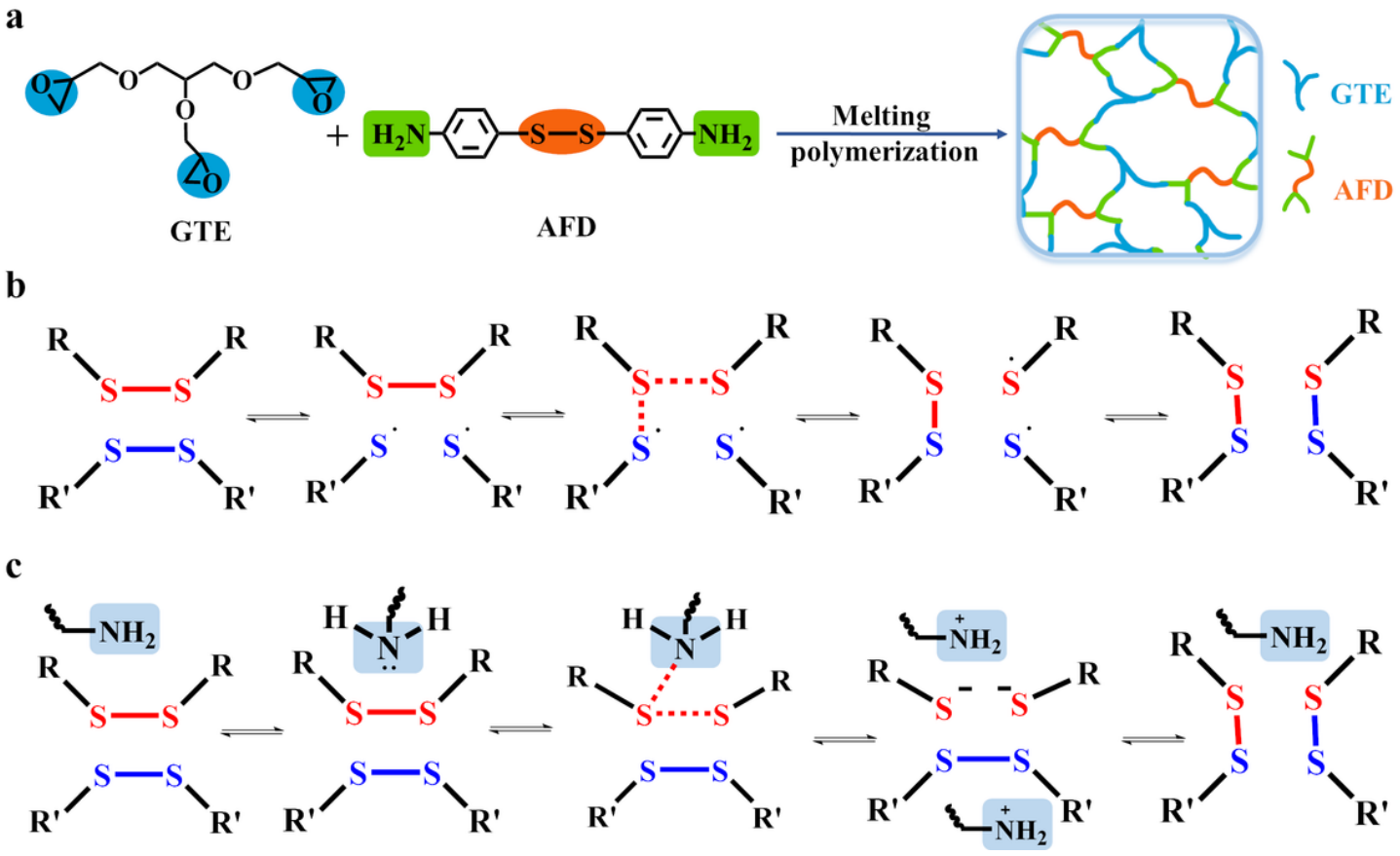

Figure 1

(a) Curing reaction, (b) [2+1] radical-mediated mechanism, (c) amino-catalyzed dynamic disulfide bond exchange mechanism

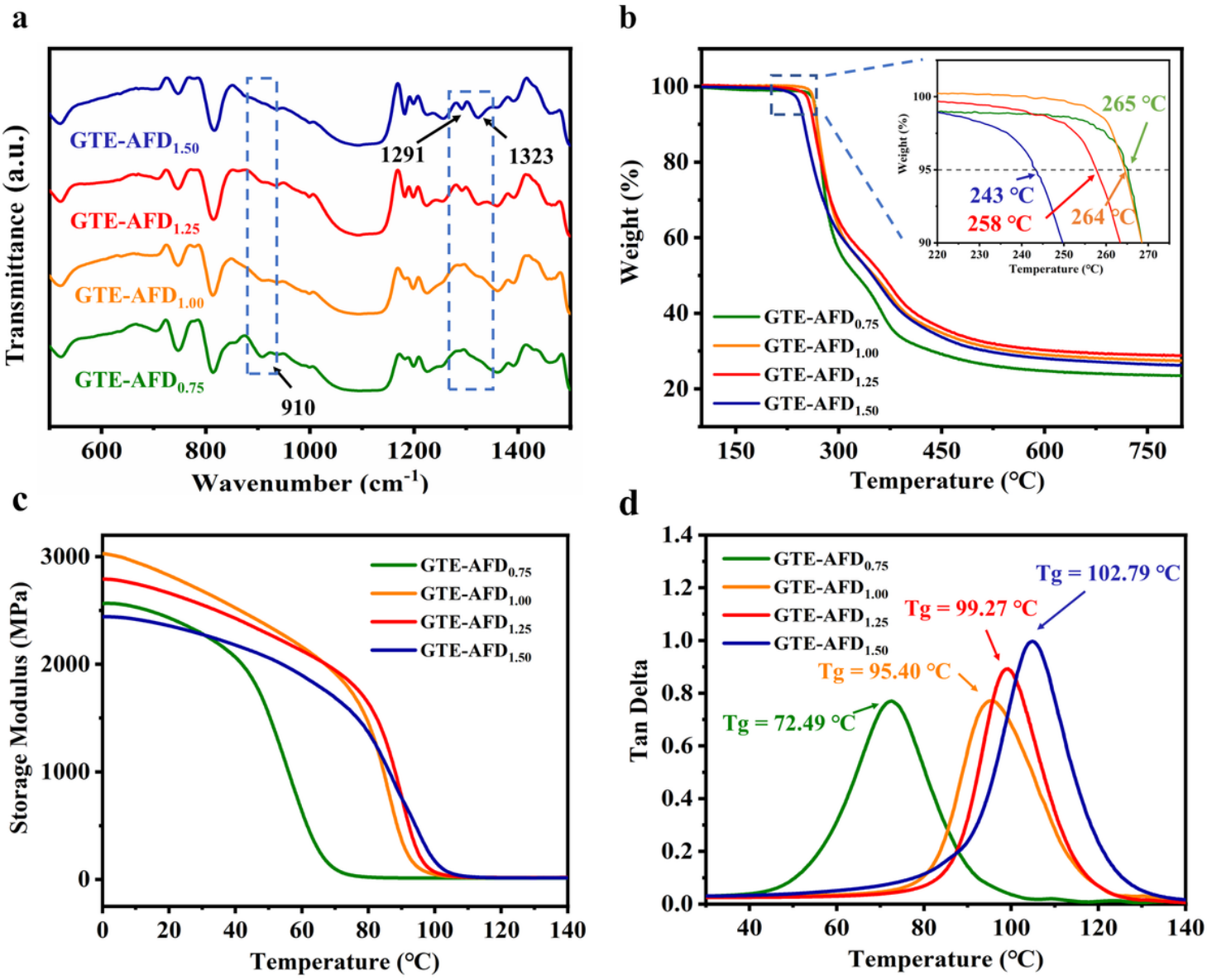

Figure 2

(a) FTIR spectra of GTE–AFD vitrimers, (b) TGA curves, (c) storage modulus curves, and (d) tan δ curves of GTE-AFD with different ratios of the AFD

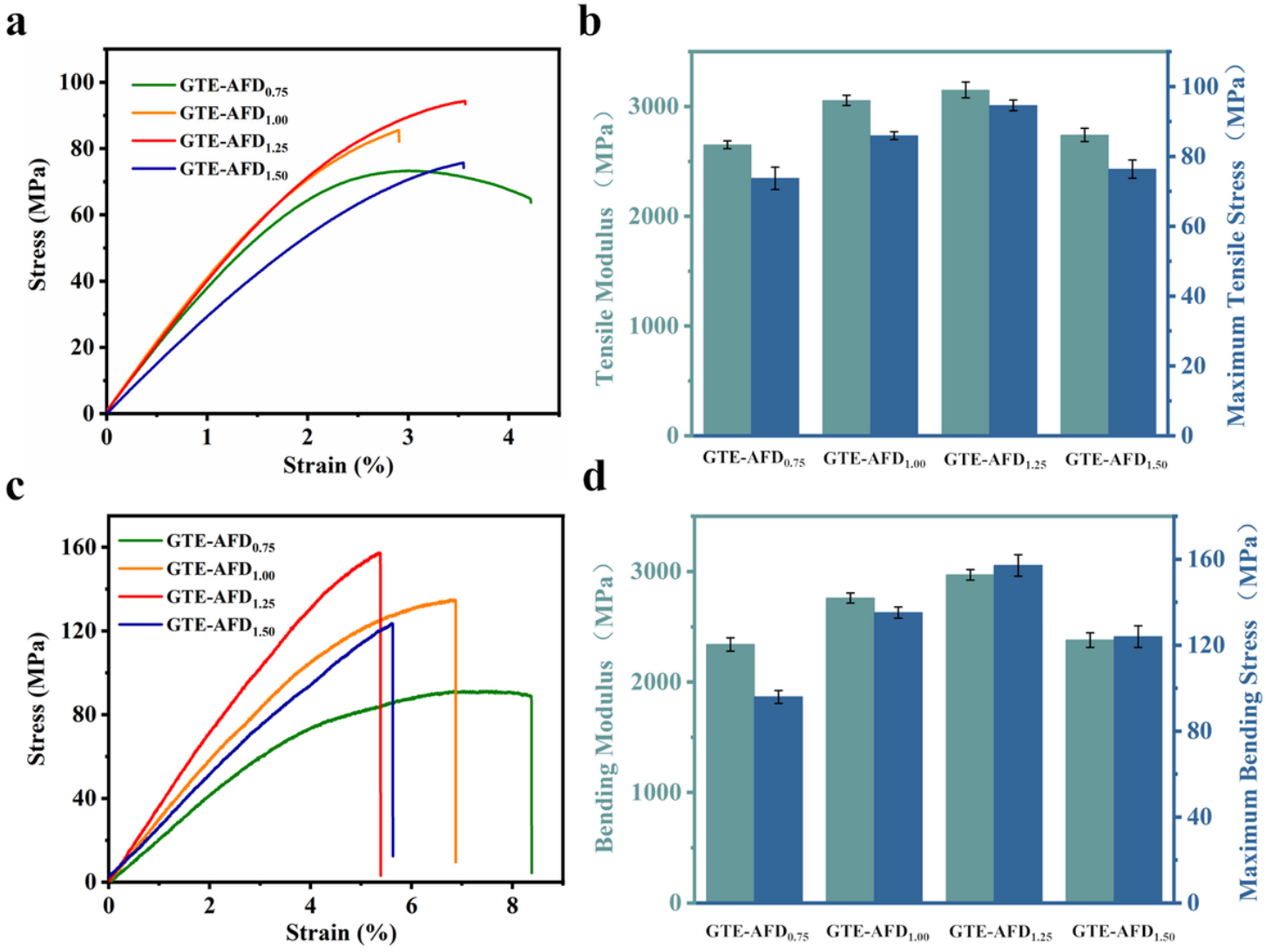

Figure 3

Typical tensile stress-strain curves (a), tensile mechanical properties (b), flexural stress-strain curves (c), and flexural mechanical properties (d) of GTE-AFD samples.

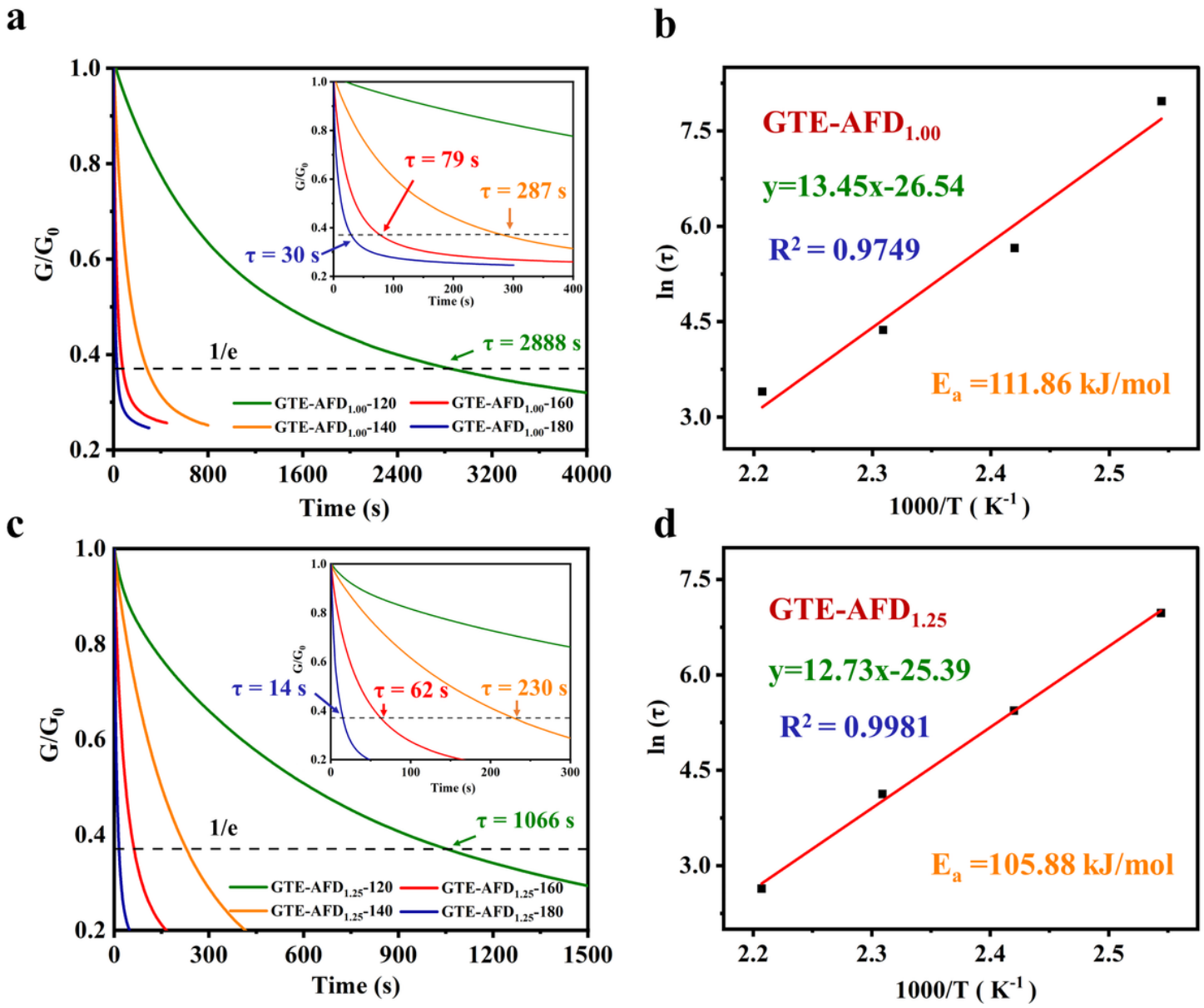

Figure 4

(a) Normalized stress relaxation curves of GTE-AFD$_{1.00}$ and (c) GTE-AFD$_{1.25}$ at 120 °C, 140 °C, 160 °C, and 180 °C, (c) ln (τ) versus 1000/T plot of GTE-AFD$_{1.00}$ and (d) GTE-AFD$_{1.25}$

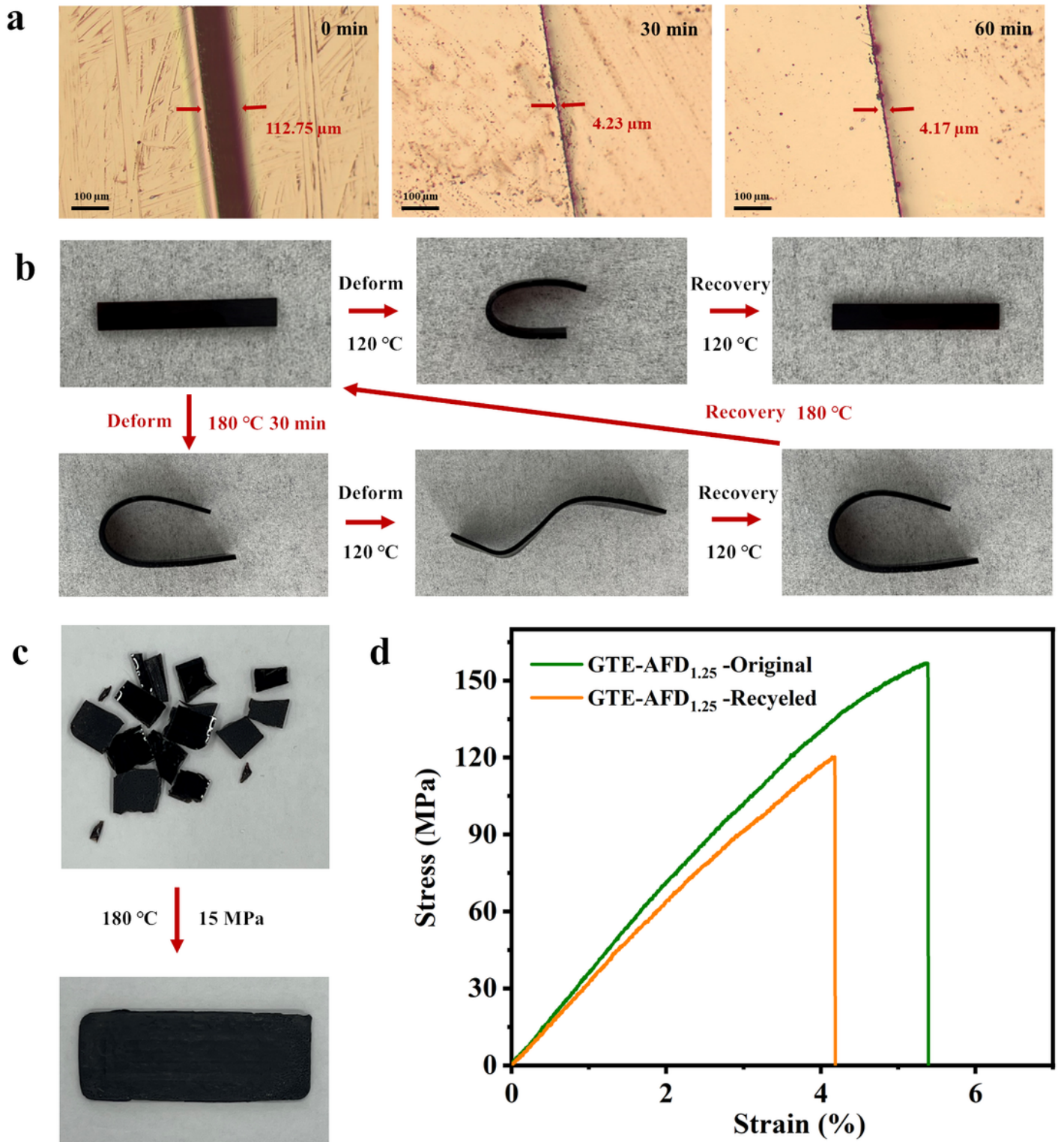

Figure 5

(a) Self-healing, (b) triple-shape memory, and (c) recycling performance photographs of GTE-AFD$_{1.25}$, (d) stress-strain curves of GTE-AFD$_{1.25}$ original and after recycled

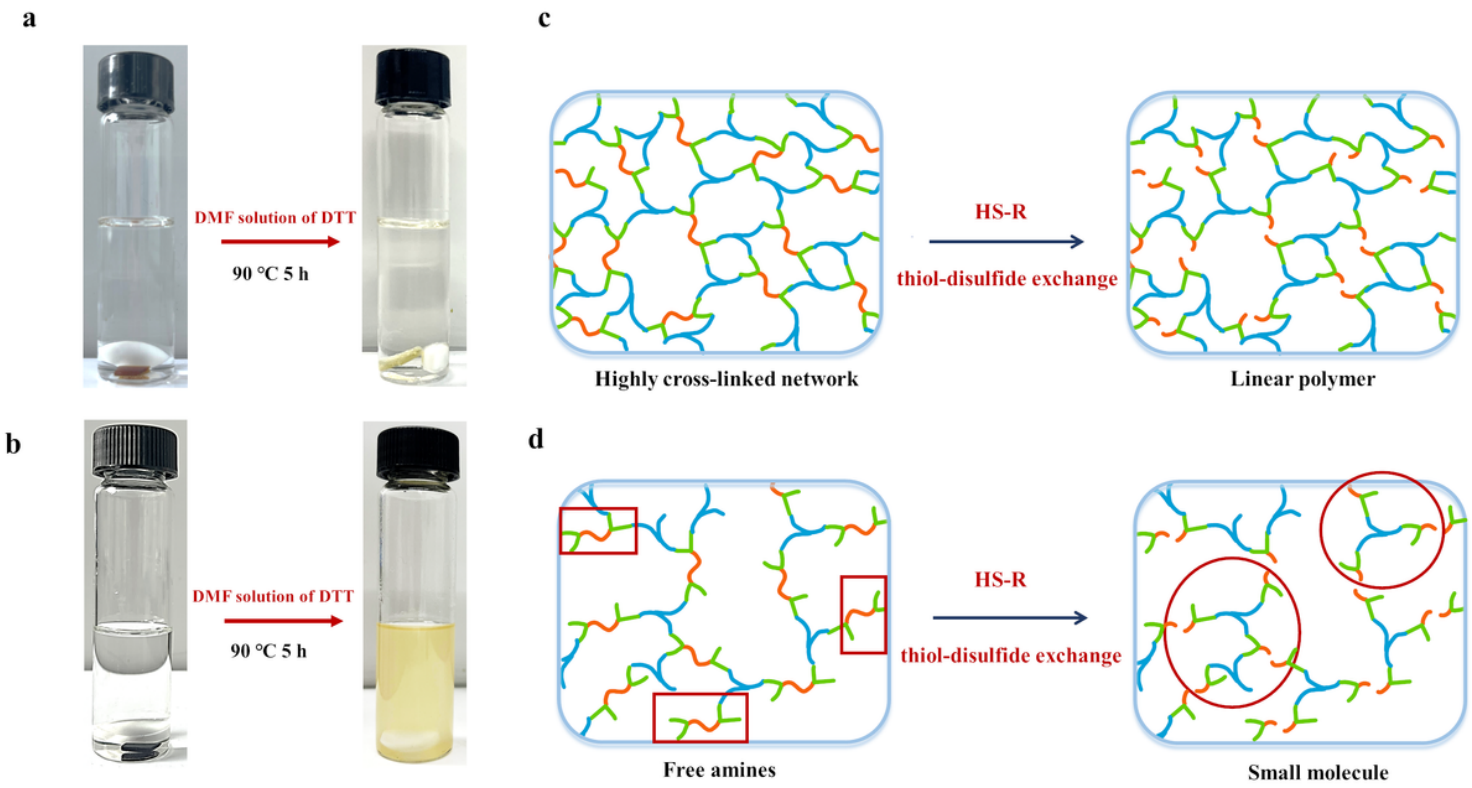

Figure 6

(a) Degradation process of GTE-AFD$_{1.00}$ and (b) GTE-AFD$_{1.25}$, (c) GTE-AFD$_{1.00}$ and (d) GTE-AFD$_{1.25}$ degradation by exchange reaction with external thiols

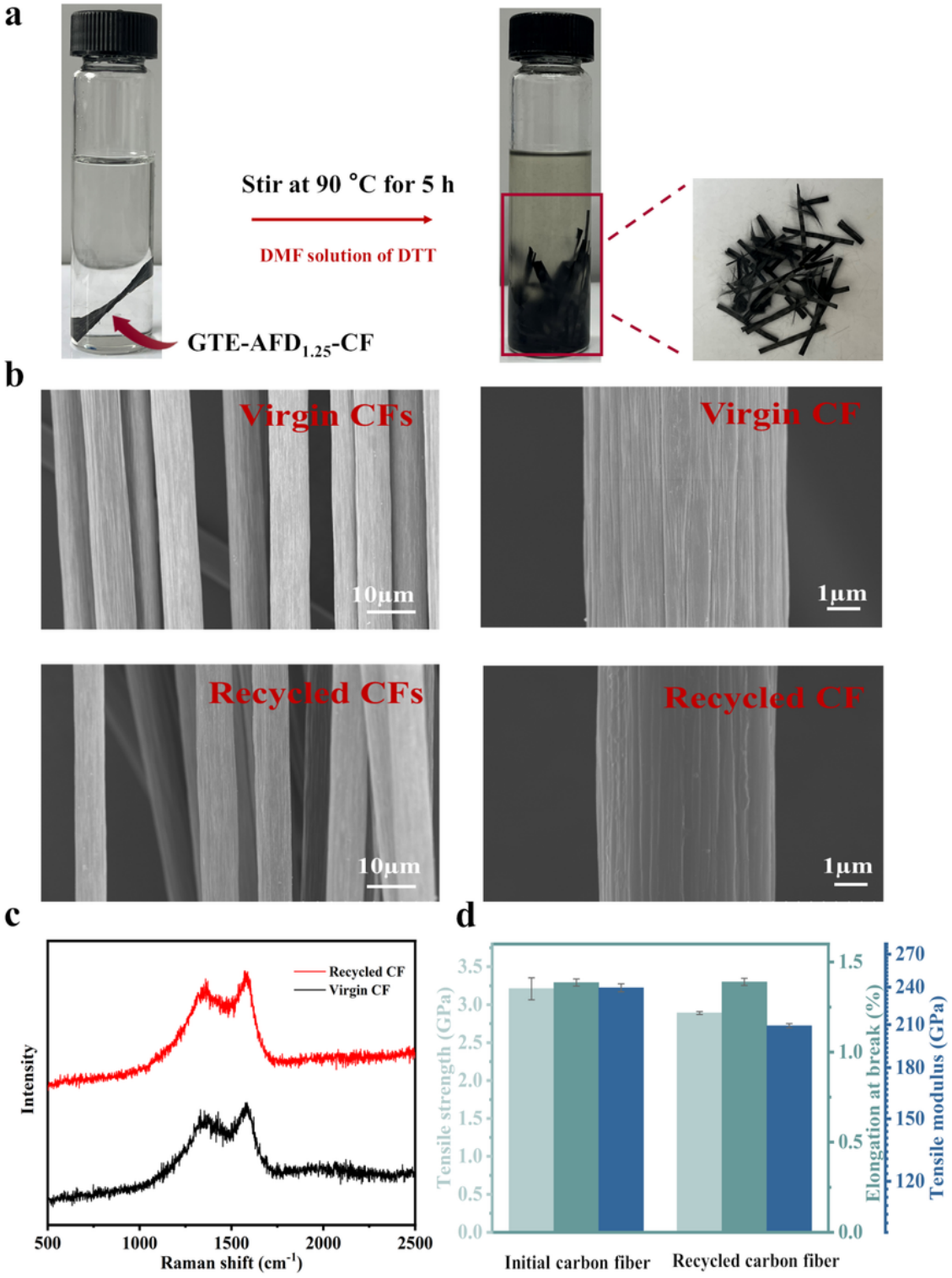

Figure 7

(a) Degradation process of GTE-AFD$_{1.25}$-CF in DMF solution of DTT, (b) SEM images of CF monofilament and CFs, (c) Raman spectra of CF monofilaments and, (d) stress-strain curves of CF monofilaments original and after recycled.

Supplementary Files

This is a list of supplementary files associated with this preprint. Click to download.

- GraphicalAbstractImage.docx
- SupportingInformation.docx